

This article was downloaded by:

On: 22 January 2011

Access details: *Access Details: Free Access*

Publisher *Taylor & Francis*

Informa Ltd Registered in England and Wales Registered Number: 1072954 Registered office: Mortimer House, 37-41 Mortimer Street, London W1T 3JH, UK



## The Journal of Adhesion

Publication details, including instructions for authors and subscription information:

<http://www.informaworld.com/smpp/title~content=t713453635>

## The Differential Displacements and the Failure in Solvent-Welded Lap Joints

C. Y. Yue<sup>a</sup>; B. W. Cherry<sup>b</sup>

<sup>a</sup> Department of Mechanical Engineering, University of Hong Kong, Hong Kong <sup>b</sup> Department of Materials Engineering, Monash University, Victoria, Australia

**To cite this Article** Yue, C. Y. and Cherry, B. W.(1987) 'The Differential Displacements and the Failure in Solvent-Welded Lap Joints', *The Journal of Adhesion*, 24: 2, 127 – 137

**To link to this Article:** DOI: 10.1080/00218468708075422

**URL:** <http://dx.doi.org/10.1080/00218468708075422>

PLEASE SCROLL DOWN FOR ARTICLE

Full terms and conditions of use: <http://www.informaworld.com/terms-and-conditions-of-access.pdf>

This article may be used for research, teaching and private study purposes. Any substantial or systematic reproduction, re-distribution, re-selling, loan or sub-licensing, systematic supply or distribution in any form to anyone is expressly forbidden.

The publisher does not give any warranty express or implied or make any representation that the contents will be complete or accurate or up to date. The accuracy of any instructions, formulae and drug doses should be independently verified with primary sources. The publisher shall not be liable for any loss, actions, claims, proceedings, demand or costs or damages whatsoever or howsoever caused arising directly or indirectly in connection with or arising out of the use of this material.

# The Differential Displacements and the Failure in Solvent-Welded Lap Joints

C. Y. YUE

*Department of Mechanical Engineering, University of Hong Kong, Pokfulam Road, Hong Kong*

B. W. CHERRY

*Department of Materials Engineering, Monash University, Victoria, Australia 3168*

*(Received November 13, 1986; in final form January 28, 1987)*

A recent analytical model for adhesive joints proposed by Yue and Cherry for analysing and predicting the strength of solvent-welded lap joints is examined. The experimental verification of an important assumed basis of the applicability of this model to solvent-welded joints is considered. The differential strain in the composite adhesive layer of the solvent-welded joint was shown to be approximately equal to the differential strain in its final adhesive layer. The differential strain and hence the stress concentration was largest near the edge of the overlap. Fractography suggested that failure of the joint initiated at the edge of the overlap.

**KEY WORDS** Joint strength; fractography; differential strain; solvent bonding; solvent welding; unplasticized PVC.

## INTRODUCTION

It is always desirable to have the capability to predict the strength or performance of adhesive lap joints before they are put into service. Unfortunately, existing analytical models cannot be generally applied since they assume failure at the maximum shear stress in the adhesive layer, an assumption which does not hold for many

adhesive systems. The current general practice<sup>1</sup> is to assume failure at the maximum shear strain.

A new analytical model for predicting the strength of solvent welded lap joints has recently been proposed by Yue and Cherry.<sup>2</sup> This new model was developed to account for the strength of solvent-welded unplasticized polyvinyl chloride (uPVC) joints which failed by rapid crack propagation. In contrast to existing models,<sup>3,4</sup> this new model assumes failure at a critical principal strain, and does not assume the stresses to be uniform across the thickness of the adhesive by considering the adhesive at the ends of the overlap to be in simple shear over a short distance. The latter assumption of non-uniform stresses across the thickness of the adhesive is in agreement with the finite element work of Crocombe and Adams.<sup>5</sup> Another difference between the existing models and the new model is that the new model predicts an increase rather than a decrease in joint strength with increasing shear modulus of the adhesive. This prediction is supported by evidence<sup>2</sup> that the increase in strength of solvent-welded joints with drying time could be attributed to the increase in modulus of the 'adhesive'.

Yue and Cherry<sup>2</sup> showed that when the effects of adherend bending are neglected, the strength of the double lap joint  $P$  could be expressed as,

$$P_f = 4b \left[ \frac{EG\eta S_1 S_2}{S_1 + S_2} \right]^{\frac{1}{2}} \frac{\epsilon_c (2 + \epsilon_c)}{(1 + \epsilon_c)} \tanh \left( \frac{\lambda l}{2} \right) \quad (1)$$

where  $b$  is the width of the joint,  $G$  the adhesive shear modulus,  $E$  the modulus of the adherends,  $l$  the overlap length,  $\eta$  with adhesive thickness,  $\epsilon_c$  the critical failure strain,  $S_1$  and  $S_2$  are the adherend thicknesses, and  $\lambda^2 = (G/E\eta)(S_1 + S_2)/S_1 S_2$ . If adherends of the same thickness,  $t$ , are utilized for the double lap joint, then  $S_1$  and  $S_2$  are defined<sup>6</sup> as  $[t - \eta/2]$  and  $[t/2 - \eta/2]$  respectively. This model can be suitably modified to account for bending stresses acting on the adhesive layer.

Yue and Cherry's model was developed from a consideration of the stress in a simple adhesive lap joint loaded in shear. However, solvent-welded joints have a more complex structure. The composite adhesive layer (CAL) in solvent-welded joints comprises<sup>2</sup> a sandwich made up of a final adhesive layer (FAL) between two

solvent-affected zones (SAZ) [*e.g.*, see Figure 1]. The FAL is the residual solvent cement layer which exists at the original interface, while the SAZs are distinct regions of the adherends that have been softened by the solvent cement. Failure always occurred within the FAL and along the SAZ/FAL interface. Yue and Cherry did not show why their model was applicable to solvent-welded lap joints which had a complex structure. They simply stated that an important assumption was that the transfer of stress across the CAL should be such that the magnitude of the differential displacement across the FAL bears a constant ratio to the magnitude of the differential displacement across the CAL at that point along the overlap. No explanation was given for the significance or meaning of the above ratio of differential displacement.

Hence, the object of the present work is to elucidate why the above new model (which was developed by considering the simple adhesive lap joint in shear) was applicable<sup>2</sup> to solvent-welded joints which had a composite adhesive structure.

## EXPERIMENTAL

The adherends (prepared from 6 mm thick calendered, unplasticized polyvinyl chloride [uPVC] sheet) and solvent cement used for preparing the double-lap joints were similar to those used in a previous work.<sup>2</sup> The double-lap joint specimens were initially 15 mm wide and were dried for 24 hours at  $23 \pm 1^\circ\text{C}$ . The width of the specimen was then reduced to 13 mm by metallographically polishing one of its sides to  $14 \mu\text{m}$  in order to expose a typical portion of the composite adhesive layer. The initial gaps between the adherends of all specimens was 0.20 mm. Specimens with overlaps of between 15 and 40 mm and SAZ ratios of between 1.0 and 3.0 were prepared for testing. The SAZ ratio is the ratio of the thickness of the SAZ in the outer adherend to the thickness of the SAZ in the central adherend of a double-lap joint. The SAZ ratio has a large effect on the joint strength and can be varied using the technique outlined elsewhere.<sup>2</sup>

The method for determining the magnitude of differential displacements was adapted from the technique used by Hennig.<sup>7</sup> Basically, 0.1 mm wide lines from a letter press lettering set were

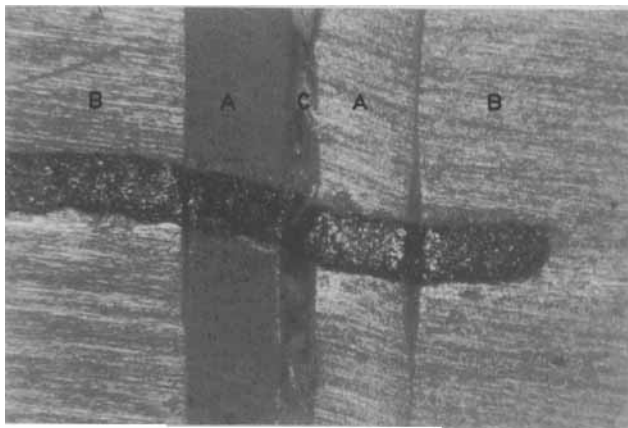


FIGURE 1 Typical photographic record of displacement of letter set line on the surface of the specimen, A-SAZ, B-adherend, C-FAL, magnification 60X.

transferred to different positions along the polished surface of the specimen such that the lines were perpendicular to the CAL. The specimen was loaded to either 200 N or 400 N and then held in tension at constant strain in an Instron testing machine. The differential displacements along the overlap could be determined from the differential displacements of the letter-set lines (Figure 1 and Figure 2) using photographic methods.

Since the specimen stress relaxed (see Figure 3), the displaced letter-set lines were photographed quickly after the specimen had been loaded for 2.5 min. All the letter-set lines along the joint

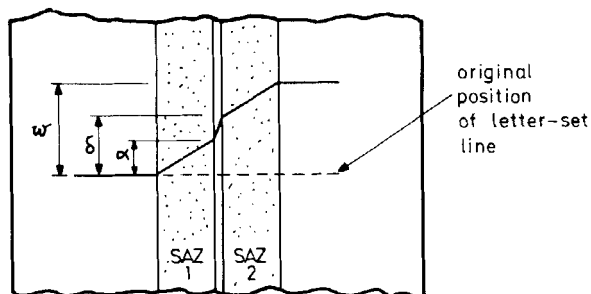


FIGURE 2 Schematic representation of method to determine displacements of lines from the photographic records. displacement of CAL =  $\delta$ , displacement of FAL =  $\delta - \alpha$ , displacement in SAZ1 =  $\alpha$ , displacement in SAZ2 =  $w - \delta$ .

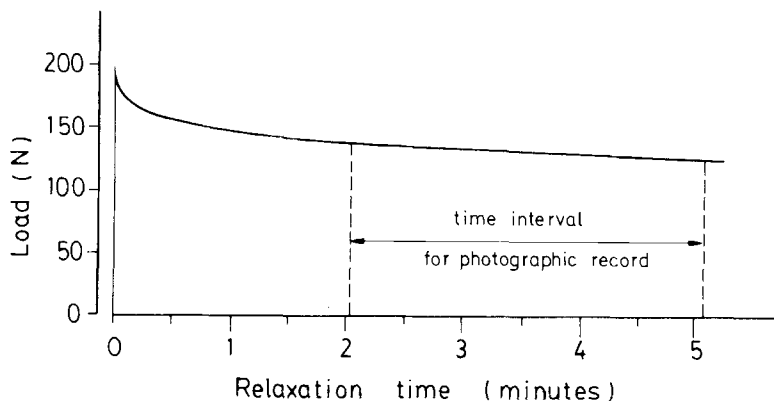


FIGURE 3 Typical stress relaxation observed in double-lap specimen at constant displacement (loading to 200 N).

overlap could be photographed within 2 min. In this way, consistent results could be obtained from the photographic records since the specimen did not relax stress much within the above period (see Figure 3). Often the non-uniform deformation of the letter press lines across the SAZ/unaffected adherend interface and across the SAZ/FAL interface caused the letter-set lines to peel off the surface of the specimen so that reliable results could not be obtained. Hence, only results from sets of lines which had not peeled from the polished surface were recorded for analysis.

Some of the double-lap specimens were tested to failure at a constant cross-head speed of 5 mm/min. The fracture surfaces of the failed specimens were sputter coated with gold and examined in a S410 Cambridge Stereoscan scanning electron microscope.

## RESULTS AND DISCUSSION

### Stress transfer in Composite Adhesive Layer

All specimens with different SAZ ratios and overlap lengths displayed typical variation of the differential displacements along the overlap similar to that shown in Figure 4. The results in Figure 4 are for half the overlap of a specimen with 32 mm overlap and an

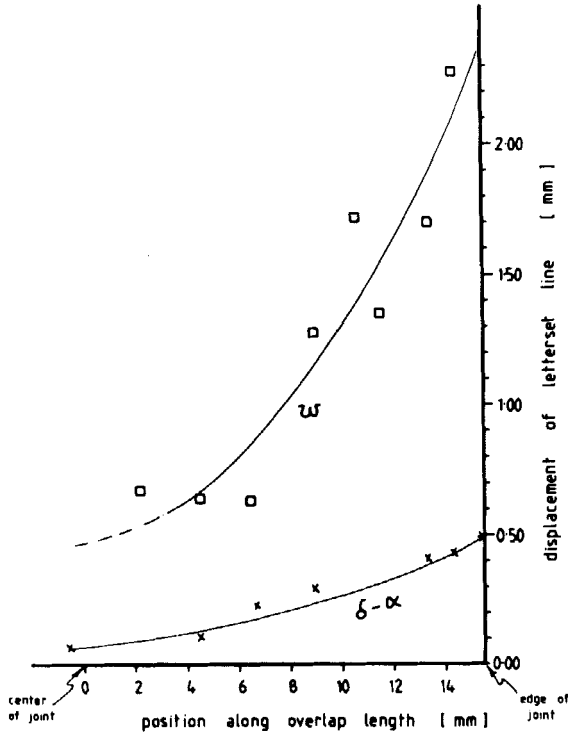


FIGURE 4 Differential displacements in the FAL and in the CAL in a specimen with an SAZ ratio of 2.0.

SAZ ratio of 2.0. The two curves in Figure 4 exhibit the same trend in that the displacements of the letter set lines in the FAL ( $\delta-\alpha$ ) and the CAL ( $\omega$ ) had minimum values at the center of the overlap and were maximum close to the edges of the overlap.

The above result indicated that there were differential displacements in both the FAL and the CAL. In agreement with the model proposed<sup>2</sup>, the strain (and by implication the stress concentration) was maximum near the edges of the overlap. The exact point of maximum strain cannot be determined from the above technique. It is interesting that for any given position along the joint overlap, the magnitude of the differential displacement in the FAL was approximately 4.5 times less than that in the CAL (Figure 4). This satisfies one of the basic assumptions for the applicability of Yue

TABLE I  
Differential displacements in 32 mm overlap specimen with SAZ ratio of 2.0 (loading to 200 N)

Distance from center of joint (mm)	Differential Displacement in		Thickness of		Shear strain ( $\times 10^{-2}$ ) in		
	CAL (mm) $\pm 7\%$	FAL (mm) $\pm 14\%$	CAL (mm) $\pm 7\%$	FAL (mm) $\pm 14\%$	CAL [SSI] $\pm 14\%$	FAL [SS2] $\pm 28\%$	SS1/SS2
4.5	0.064	0.011	2.100	0.268	3.0	4.1	0.73
9.0	0.179	0.029	2.143	0.268	8.4	10.8	0.78
13.4	0.215	0.041	1.741	0.223	12.3	18.4	0.67
14.3	0.229	0.043	1.741	0.223	13.2	19.3	0.68
15.4	0.234	0.050	1.518	0.268	15.4	18.7	0.82

and Cherry's model to solvent-welded joints. The implication and significance of the above assumption will now be examined.

The shear strains in the CAL and the FAL at different positions along the overlap for the data in Figure 4 are given in Table I. From Table I it can be seen that the shear strain in the CAL approaches that in the FAL along the entire overlap. Similar calculations for data from a specimen with 35 mm overlap and an SAZ ratio of 1.0 are shown in Table II. From Table II it is evident that the shear strain in the CAL is also approximately equal to the shear strain in the FAL along the entire overlap. Other specimens also yielded similar results. It is clear from the above observations that the magnitude of the shear strain in the CAL at any point along the overlap was probably equal to the magnitude of the shear strain in

TABLE II  
Differential displacements in 35 mm overlap specimen with SAZ ratio of 1.0 (loading to 400 N)

Distance from center of joint (mm)	Differential Displacement in		Thickness of		Shear strain ( $\times 10^{-2}$ ) in		
	CAL (mm) $\pm 7\%$	FAL (mm) $\pm 14\%$	CAL (mm) $\pm 7\%$	FAL (mm) $\pm 14\%$	CAL [SSI] $\pm 14\%$	FAL [SS2] $\pm 28\%$	SS1/SS2
1.7	0.318	0.043	0.953	0.159	0.334	0.270	1.24
2.6	0.363	0.054	0.998	0.159	0.364	0.340	1.07
4.4	0.397	0.039	1.225	0.102	0.324	0.382	0.85
7.9	0.454	0.073	1.202	0.193	0.378	0.278	1.00
15.7	0.499	0.102	1.315	0.249	0.379	0.410	0.92
17.0	0.567	0.102	1.429	0.227	0.397	0.449	0.88



the FAL at that point for all solvent-welded joints irrespective of the SAZ ratio. This is why Yue and Cherry's model (which was developed for simple adhesive lap joints and which would only enable one to calculate the shear strain in the CAL and not in the FAL) is applicable to solvent-welded joints which have a more complex structure.

### Failure in solvent welded joints

Typical fractographs along the overlap of the specimens are as shown in Figures 5 and 6. In general, the appearance of the fracture surface did not depend on the specimen overlap length. The fractographs in Figures 5 and 6 were taken from specimens with overlap lengths of 40 mm and 35 mm respectively. Only the fractographs for regions up to half the overall overlap length away from the leading edge of the joint are provided. The appearance of the fracture regions which were equidistant from the center of the joint (in the direction of the joint overlap) were very similar.

The micrographs in Figure 5 revealed that the polymer in the final adhesive layer near the center of the overlap (5C) was not as extensively deformed as that located nearer the edge (5B). Entrapped air bubbles were sometimes present near the edge of the overlap. Such an entrapped air bubble within the overlap can be seen near the top right of Figure 5A. (The entrapped air bubble is the elliptical hole at the top right corner which extends to the center right of the micrograph) In Figure 5A, the edge of the overlap is located just above the entrapped air bubble. It can be seen that the

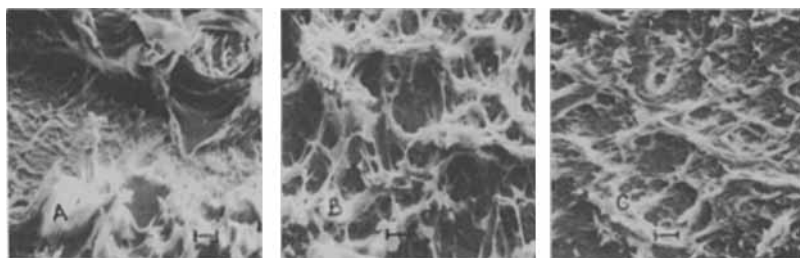


FIGURE 5 Typical fractographs along the failure surface of a double-lap specimen with 40 mm overlap [Benchmark 20  $\mu\text{m}$ ]. A—Region close to edge of overlap, B—Region farther away from edge of overlap, C—Region near centre of overlap.

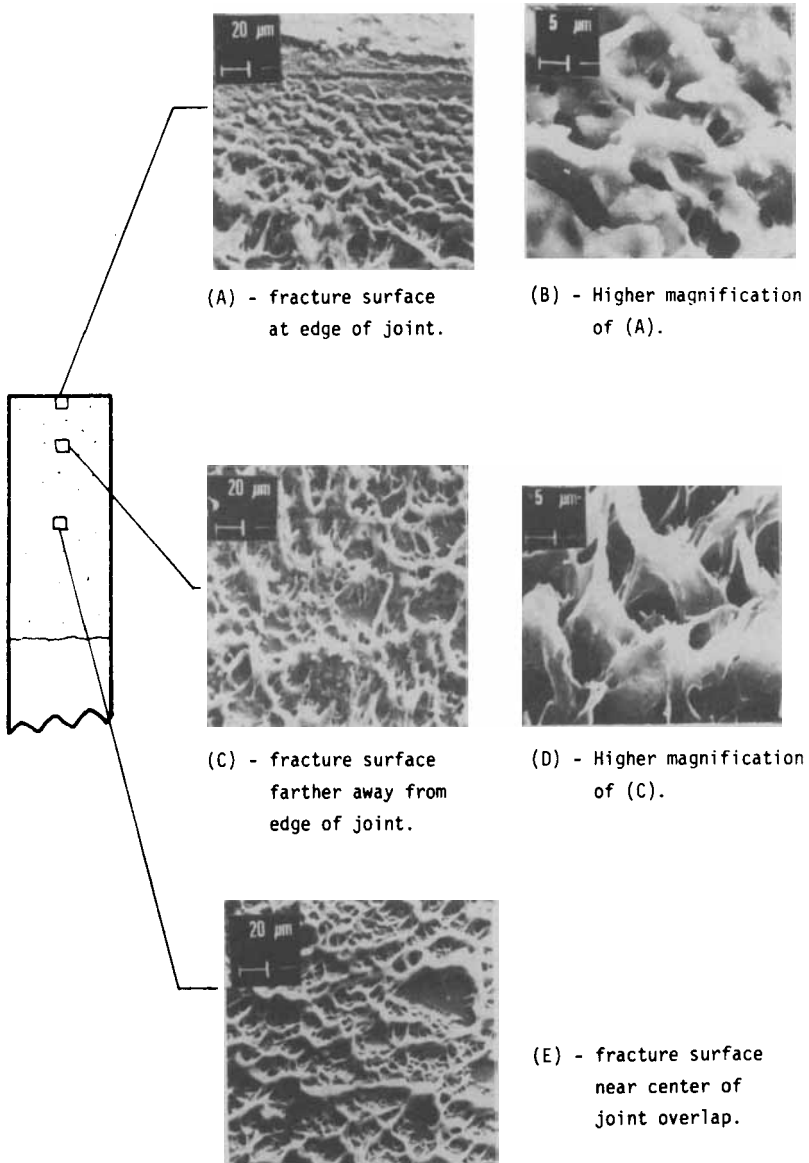


FIGURE 6 Typical fractographs along the failure surface of a double-lap specimen with 35 mm overlap.

polymer near the edge of the overlap, typified by the region in the lower half of Figure 5A, was more extensively deformed than the polymer in either Figures 5B or 5C. Therefore, the micrographs in Figure 5 revealed that the polymer within the final adhesive layer was increasingly more deformed and extended as one moved from the center to the edge of the joint. The above trend was also observed along the fracture surface of the overlap in Figure 6. Occasionally, at the edge of the overlap, features similar to that shown in Figure 6A exist next to areas which exhibited features shown in the lower half of Figure 5A. The fracture surface in Figure 6A appears to be made up of extensively deformed polymer (similar to that in Figure 5A) that had melted. Comparison of Figures 6B and 6D, which are higher magnifications of the fracture surfaces in Figures 6A and 6C respectively, did indeed strongly suggest that the polymer at and near the edges of the joint had probably melted after undergoing extensive plastic deformation. The fact that melted (Figure 6A) or the most extensively deformed polymer (Figure 5A) was located at or very near the leading edge of the overlap probably indicated that failure of the solvent-welded joint in shear was initiated at the edges and that differential strains exist in the FAL prior to failure.

Polymer melting associated with rapid rises in temperature has been observed by Kambour and Barker<sup>8</sup> where the craze propagation velocity in polymethyl methacrylate was between 100 and 1000 mm/sec. The crack propagation speed during the rapid failure of the solvent-welded uPVC specimens was estimated to be in excess of 100 mm/sec from the load extension charts. Hence, it is possible that polymer melting may have occurred in the specimens. No further evidence of polymer melting was sought since this subject is outside the scope of the present work. The important point is that, in agreement with Yue and Cherry's model, failure in the solvent-welded specimens initiated at the edges of the overlap.

## CONCLUSIONS

The differential displacement experiments revealed that, in solvent-welded joints, the maximum shear strain in the CAL was

equal to the maximum shear strain in the FAL. Thus Yue and Cherry's model, which was developed from a consideration of the simple lap joint and which permitted the calculation of the strains in the CAL, was applicable to solvent-welded joints which had a complex structure. Fractography indicated that, in agreement with Yue and Cherry's model, failure in the solvent-welded joints initiated at the edge of the overlap.

### Acknowledgement

Some of the experimental work was conducted at Monash University for which Professor I. J. Polmear is thanked for provision of laboratory facilities. The rest of the work was carried out in Hong Kong.

### References

1. A. J. Kinloch, *J. Mat. Sci.* **17**, 617 (1982).
2. C. Y. Yue and B. W. Cherry, in *Adhesion* 10, K. W. Allen, Ed. (Elsevier Appl. Sci. Publ., London, 1986), pp. 147-177.
3. O. Volkersen, *Luftfahrtforschung* **15**, 41 (1938).
4. M. Goland and E. Reissner, *J. Appl. Mech. Trans. ASME* **66**, A17 (1944).
5. A. D. Crocombe and R. D. Adams, *J. Adhesion* **13**, 141 (1981).
6. C. Y. Yue and C. M. Chui, submitted to *J. Adhesion*.
7. G. Hennig, *Plaste u Kaut.* **12**, 159 (1965).
8. R. P. Kambour and R. E. Barker, Jr., *J. Polym. Sci. Part A2* **4**, 359 (1966).